Accepted Manuscript

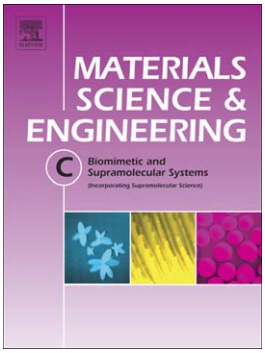

Changes induced by UV radiation in the presence of sodium benzoate in films formulated with polyvinyl alcohol and carboxymethyl cellulose

S. Villarruel, L. Giannuzzi, S. Rivero, A. Pinotti

PII: S0928-4931(15)30190-9
DOI: doi: 10.1016/j.msec.2015.07.003
Reference: MSC 5574

To appear in: *Materials Science & Engineering C*

Received date: 12 August 2014
Revised date: 21 May 2015
Accepted date: 8 July 2015

Please cite this article as: S. Villarruel, L. Giannuzzi, S. Rivero, A. Pinotti, Changes induced by UV radiation in the presence of sodium benzoate in films formulated with polyvinyl alcohol and carboxymethyl cellulose, *Materials Science & Engineering C* (2015), doi: 10.1016/j.msec.2015.07.003

Changes induced by UV radiation in the presence of sodium benzoate in films formulated with polyvinyl alcohol and carboxymethyl cellulose

S.Villarruel[b], L.Giannuzzi[a], S.Rivero[a] and A.Pinotti[a,c,*]

[a]Center for Research and Development in Food Cryotechnology (CCT-CONICET La Plata), 47 and 116.

[b]Faculty of Exact Sciences, UNLP.

[c]Faculty of Engineering, UNLP, La Plata (1900), Argentina.

Abstract

This work was focused on: i) developing single and blend films based on carboxymethyl cellulose (CMC) and polyvinyl alcohol (PVOH) studying their properties, ii) analyzing the interactions between CMC and PVOH and their modifications UV-induced in the presence of sodium benzoate (SB), iii) evaluating the antimicrobial capacity of blend films containing SB with and without UV treatment.

Once the blend films with SB were exposed to UV radiation, they exhibited lower moisture content as well as and a greater elongation at break and rougher surfaces compared to those without treatment. Considering oxygen barrier properties, the low values obtained would allow their application as packaging with selective oxygen permeability. Moreover, the characteristics of the amorphous phase of the matrix prevailed with a rearrangement of the structure of the polymer chain, causing a decrease of the crystallinity degree. These results were supported by X-rays and DSC analysis. FT-IR spectra reflected some degree of interaction polymer-polymer at molecular level in the amorphous regions. The incorporation of sodium benzoate combined with UV treatment in blend films was positive from the microbial point of view because of the growth inhibition of a wide spectrum of

microorganisms. From a physicochemical perspective, the UV treatment of films also changed their morphology rendering them more insoluble in water, turning the functionalized blend films into a potential material to be applied as food packaging.

Key words: sodium benzoate, blend films, UV radiation, CMC, PVOH, antimicrobial capacity

Corresponding author: acaimpronta@hotmail.com (A.Pinotti)

Introduction

Among cellulose ethers, a most widely used is carboxymethyl cellulose (CMC) produced in the form of sodium salt. The CMC structure is based on the 1,4-β-Dglucopyranose polymer of cellulose. Cellulose derivatives have been used to develop cellulose-based hydrogels through physical and chemical cross-linking [1-3]

On the other hand, polyvinyl alcohol (PVOH), a semi-crystalline polymer is among the most widely used synthetic water-soluble polymers. This polymer is extensively produced for its excellent chemical resistance, physical properties and complete biodegradability, which has led to broad practical applications [4, 5]. PVOH has been used in polymer blends with natural polymeric materials such as cellulose derivative and chitosan. In these systems, good material performance was obtained, which is attributable to the formation of intermolecular hydrogen bonds between the hydroxyl groups of the respective polymers [6]. The blend of two polymers allows the preparation of polymeric materials with controllable properties differing significantly from those of the individual components [7].

In so doing, blends of CMC and PVOH have been the subject of a number of investigations [8-10, 4, 11-14]. The mixture of these polymers enables the production of biodegradable materials with physical and functional properties, allowing their application in the emerging field of packaging.

The photo-curing technique has proved to be an important method for cross-linking polymers because their functional groups undergo light induced reactions [15, 16], being used to improve the properties of the matrices associated to the chemical reaction [17]. Modifications by using UV radiation of polymer films have been studied in recent years [17-19].

UV radiation requires the presence of substances known as photosensitizers which induce the changes in the substrate after absorbing appropriate radiation.

Chen and Lin [20] found that the modification of PVOH can be carried out by UV radiation in the presence of photosensitizers or by chemical reactions. These processes can lead to the cross-linking of PVOH molecules, making the polymer more insoluble in water. The most efficient photosensitizer is sodium benzoate (SB), known to be photolysed by UV radiation [21, 22]. Excitation of photoinitiator produces reactive radicals which initiate subsequent reactions in the polymer blend thus facilitating cross-linking between the two polymer chains [16].

Other use of SB is focused on the preservation of food matrices because of its antimicrobial capacity, extending its functionality and its spectrum of application. SB is the most common, safe, food preservative and antimicrobial agent classified in the United States as Generally Recognized as Safe (GRAS) [23].

To the best of our knowledge, the use of UV light to induce the photo-crosslinking of PVOH:CMC blend films in the presence of SB has hardly been reported. Thus, new materials with tailored properties from PVOH and CMC blends were expected to be found.

This work was focused on:

i) Developing single and blend films based on carboxymethyl cellulose and polyvinyl alcohol analyzing their properties.

ii) Studying the ultraviolet-induced cross-linking of blend films with SB in order to alter their surface properties and introduce new functionalities, evaluating the changes undergone by the blend because of the addition of the photo-iniciator by using SEM and DMA techniques.

iii) Evaluating the antimicrobial capacity of blend films containing SB with and without UV treatment.

Thus, microstructural, physical, optical and thermal properties were monitored for single, blend films and UV crosslinked matrices.

Materials and Methods

Reagents

Sodium carboxymethyl cellulose of commercial grade was supplied by Parafarm (Buenos Aires, Argentina) with a degree of substitution of 0.95. Polyvinyl alcohol ELVANOL ® T25 was purchased from DuPont (Buenos Aires, Argentina) with a hydrolysis degree of 86-89 %. Sodium benzoate, supplied by SUPELCO Analytical (USA), was used as a photosensitizer.

Film-forming solution and film preparation

CMC aqueous solution was prepared by dispersing 1.5 % (w/w) of the polymer in stirred distilled water at 80ºC, for 12 h approximately. Then, the beaker containing the solution was sonicated for 30 minutes to remove the air bubbles at room temperature.

PVOH solution of 2 % (w/w) was obtained by solubilization in water at 90°C under continuous agitation for 45 min approximately.

In previous work, solutions with different ratios of CMC:PVOH (25:75, 50:50, 75:25) were tested [24]. The blend 50:50 (w/w) was selected for further studies owing to its better barrier and mechanical properties, bearing in mind that it would be used as a functional active film. Blend films containing SB as a photosensitizer for the crosslinking reaction were also prepared. With the purpose to meet the required amounts for a potential application as packaging where the films are in contact with food products, the concentration of SB was fixed at 0.1%, according to the current norm [25].

Single CMC, PVOH and their blends were prepared by casting 25 g of filmogenic solutions onto Petri dishes (9 cm diameter) and drying at 37°C in an oven until reaching constant weight (approximately 36 h). Film thickness was determined using a coating thickness gauge Check Line DCN-900 (New York, USA) for non-conductive materials on non-ferrous

substrates. The informed values correspond to the average of at least fifteen measurements at different positions for each specimen.

Films were conditioned in a controlled room at 20°C and 65% relative humidity (RH) before doing the analyses. From here onwards, blend films with the addition of SB will be also named CMC:PVOH/SB.

UV-treatment

In this study the matrices underwent a photochemical treatment as a result of UV curing in solid state (film). The blend films with SB were placed in plastic supports under a bank of mercury lamps, which emits light mainly of 254 nm wavelength (TUV G30T8, 30W, Philips, Bs. As., Argentina). The intensity of radiation was 0.14 J cm^{-2} min, obtaining different doses by altering the duration of the exposure at a fixed distance. The dose of incident radiation was 11 and 22 J cm^{-2} during 80 and 160 min, respectively. Blend films were rotated to expose each side to radiation.

The radiation intensity was measured with an UV digital Radiometer (Model WLX3W, Cole-Palmer Instrument Company, Vernon Hills, IL, USA). All measurements were performed in the same conditions of temperature and humidity to avoid any influence on the physicochemical properties of films.

Blend films with the addition of SB exposed to UV radiation and CMC:PVOH/SB UV will be used as synonymous.

Film properties

Moisture content

Film moisture contents were determined by measuring their weight loss, upon drying in an oven at 105±1ºC until reaching constant weight (dry sample weight). Samples were analyzed at least in triplicate and results were expressed as grams of water per 100 g of sample.

Optical properties

Film opacity was determined by using the procedure described by Cho and Rhee [26] and film transparency was determined following the method described by Zhang and Han [27]. Film samples were cut into a rectangle and placed on the internal side of a spectrophotometer cell. The absorption spectra of films were recorded in the wavelength range 200–700 nm by using a UV-visible Spectrophotometer (Hitachi U 1900, Japan).

Film opacity was defined as the area under the recorded curve determined by an integration procedure between 400 and 700 nm. The opacity was expressed as absorbance units per nanometers (AU). Film transparency was calculated by the ratio between the absorbance at 600 nm (A_{600}) and film thickness, being expressed as A_{600} mm^{-1}. The measurement was repeated three times for each type of film, and the average value was informed.

Film solubility and swelling

To determine film solubility, the samples were cut in 3×3cm pieces, weighed and placed into test beakers with 80 ml deionizated water. The samples were maintained under constant agitation for 1 hour at 20°C. The remained pieces of the films after soaking were dried again in an oven at 105±1ºC to a constant weight. Film solubility (%) was calculated as follows:

$$\%\,\text{Solubility} = \left[\frac{(\text{Initial dry weight} - \text{Final dry weight})}{\text{Initial dry weight}}\right] \times 100 \qquad \text{Eq. (1)}$$

Swelling was measured by immersion of previously weighted film pieces in 80 ml distilled water. After 60 min of hydration, the samples were recovered and dried with filter paper to remove the excess of surface water and weighted (weight of swollen sample). The swelling of the films was calculated according to the following equation, where Wt is the weight of the swollen sample at time t and Wi is the weight of the dried film:

$$\%\,Water\ \text{uptake} \quad = \quad \left[\frac{(W_t \quad - \quad W_i)}{W_i}\right] \times 100 \qquad \text{Eq. (2)}$$

Samples were analyzed at least in triplicate.

Water vapor permeability

Water vapor permeability (WVP) tests were conducted based on a modified ASTM method E96 [28] using a specially designed permeation cell that was maintained at 20°C as described in previous work. After steady-state conditions were reached, eight measurements were performed over 8 h. Each informed value corresponded at least to four determinations.

Oxygen transmission measurements

Oxygen barrier properties of films were carried out using a MOCON OX-TRAN Model 2/21 (Mocon Inc., Minneapolis, USA) gas permeability tester in accordance with the ASTM standard D3985-06 using the coulometric method. The samples were tested at 760 mm Hg, and 23°C with a 65 % relative humidity for all samples.

The test cell was composed of two chambers separated by the film. Nitrogen containing 2% of hydrogen was used as the carrier gas and pure oxygen was used as the test gas. Prior to testing, specimens were conditioned in nitrogen/hydrogen (N_2/H_2) inside the unit for at least 6 h to remove traces of atmospheric oxygen. Subsequently, oxygen was introduced in the upstream compartment of the test cell. Oxygen transferred through the film was conducted by

the carrier N_2/H_2 gas to the coulometric sensor. The oxygen permeability was expressed as $cm^3\ m^{-1}\ s^{-1}\ Pa^{-1}$.

Mechanical properties

Quasi-static test in uniaxial condition assays were conducted in a dynamic-mechanical thermal equipment Q800 (TA Instruments, New Castle, USA) using a clamp tension. A preload force of 1 N and a constant force ramp rate of 0.3 N min^{-1} were applied to record the stress-strain curves until rupture from film sample strips or up to 18 N. Tests were carried out at 25ºC. In order to calculate the elastic modulus at large deformations (E_C), stress-strain curves were fitted to Eq. (3):

$$\sigma_V = E_C\, \varepsilon_V\, e^{-\varepsilon_V K} \qquad \text{Eq. (3)}$$

where,

ε_v and σ_v are the true strain and the true stress, respectively, E_C is the elastic modulus; K is a constant and it is regarded as a fitting parameter. From Eq. (3), the relationship between the stress (σ_v) and the true deformation (ε_v) corresponds to the elastic module. Samples were analyzed at least in triplicate.

Supplementary studies on mechanical properties of films were performed in a texturometer TA.XT2i—Stable Micro Systems (England) as it was described in a previous work [29] using a tension grip system A/TG at a constant rate of 1 mm/s. Film probes of 6 cm length and 0.7 cm width were used. From curves force (N)-deformation (mm), recorded by the Texture Expert Exceed software, and considering the thickness and the dimensions of probes, stress-strain profile were obtained. Each informed value corresponded at least to six determinations.

Modulated differential scanning calorimetry (MDSC)

Modulated differential scanning calorimetric studies were performed over a temperature range of -100 ºC to 250 ºC using a DSC model Q100 controlled by a TA 5000 module (TA Instruments, New Castle, Delaware, USA), with a quench-cooling accessory, under a N_2 atmosphere (20 ml min^{-1}) and modulated capability.

The first scan was performed from -100ºC up to 200ºC. After the first scan was completed, the sample was cooled until -100°C and then a second scan was recorded.

From the thermograms the following information was obtained: T_m, the peak melting temperature (°C), ΔH, the enthalpy (J g^{-1}, dry basis). The total, reversing and non-reversing signals were determined. Crystallinity degree (CD) was estimated from the enthalpy of melting (ΔH_m) deduced by integration of the area under the melting peak and taking into account the corresponding value of ΔH_0= 138.6 J g^{-1} reported for 100% crystalline PVOH [5, 30], as follows:

$$CD = \frac{\Delta H_m}{\Delta H_0} \times 100 \qquad \text{Eq. (4)}$$

The analysis of the thermograms was performed by using the Universal Analysis V1.7F software (TA Instruments).

Structural studies through microscopic studies

Morphology of films was studied by scanning electron microscope (SEM) with a FEI model Quanta 200 electron microscope (The Netherlands). Single component and blend films were cryogenically frozen in liquid nitrogen.

Dynamic mechanical analysis (DMA)

DMA assays were conducted in dynamic-mechanical thermal equipment previously described using a clamp tension with a liquid N_2 cooling system as described in a preliminary study. Multi-frequency sweeps (1, 3, 5, 10 and 15Hz) at a fixed amplitude (15 μm) from -90 to 200ºC at 5ºC min^{-1} were carried out, with an isotherm of 15 min at -90ºC.

X-ray diffraction

CMC and PVOH powders and films were analyzed by X-ray diffraction in an X'Pert Pro P Analytical Model PW 3040/60 (Almelo, The Netherlands). The CuKα radiation (1.542 Å), operated at room temperature, was generated at 40 kV and 30 mA, and the relative intensity was recorded in the scattering range of (2θ) 3–60º with step size of 0.02°.

The area of the crystalline peak diffraction (AP) relative to the total area of the diffractogram (AT) was determined and the crystallinity degree (CD) was calculated as follows:

$$CD = \frac{AP}{AT} \times 100 \qquad \text{Eq. (5)}$$

A similar procedure was described by different authors [31-33].

FT-IR spectroscopy

The Fourier transform infrared (FT-IR) spectra of the films were recorded in an IR spectrometer (Nicolet, iS10 Thermo Scientific, Madison, USA) in the wavenumber range 4000-400 cm^{-1} by accumulation of 64 scans at 4 cm^{-1} resolution. Data were analyzed by using the software Omnic 8 (Thermo Scientific).

Antimicrobial capacity

Inoculum preparation

Isolates of *E. coli* (ATCC 25922), *Salmonella* spp. and *Penicillium* spp. were obtained from Microbiology Chair (University of La Plata, Argentina). *Candida* spp. was obtained from yeast collection of Microbiology Laboratory of CIATI (Center for Research and Technical Assistance to Agri-food Industry).

Candida spp. was growth in broth malt containing malt extract (1%, Biokar, France), yeast extract (2%, Biokar, France) and glucose (1%, Merck, Germany). *E coli* and *Salmonella* spp were grown in a nutrient broth (Merck, Germany). All culture were incubated at 37ºC for 12 hours until reaching concentrations of 10^8 CFU ml^{-1} determined by optical density (OD). Then, dilutions 1:10 were prepared from these inocula with sterile 0.1 % of peptone water (Oxoid) to obtain concentrations of 10^7 CFU ml^{-1}.

The inoculum of *Penicillium* spp. was prepared by growing the fungi on agar potato dextrose agar slants (Merck, Germany) for 7 days at 30ºC. After incubation, 10 ml of 0.01% (w/v) sodium lauryl sulfate (Merck, Germany) in 1% (w/w) sodium chloride solution were added to the tubes and spores were loosened by gently scraping with a spatula, and serial dilutions were made [34]. The cells were counted in a haemocytometer and diluted to a concentration of 10^5 spores ml^{-1}. Besides, a dilution 1:10 was also prepared with sterile 0.1% of peptone water (Oxoid).

Antimicrobial test

The antimicrobial capacity of the active films was determined by using the agar diffusion method described by Rivero et al. [35].

The inocula previously described were tested using 3 cm diameter film discs which were placed by pressing them to ensure contact with the agar surface. The average thickness of the studied films was 45µm.

The discs were deposited on petri dishes of 9 cm diameter with Nutrient agar (Merck) for trials with *E coli* and *Salmonella* spp. and with Agar Malta (malt extract 1%, yeast extract 2%, glucose 1% and agar 2%) for *Candida* spp. and *Penicillium* spp. previously planted from 100 µl of the corresponding inoculum. The tests were performed in duplicate to ensure reproducibility of the results. Visual observations were conducted in all cases, photographs were taken, and inhibitory zones of the films were observed at 24 h of incubation at 37°C.

Inhibition percentage was defined as the inhibition zone in relation to the total area of petri dishes. Observations of the diameter of the inhibitory zone surrounding film discs and the contact area of edible film with the medium surface were made. The photographs were processed with software Image J.

Statistical analysis

Systat-software (SYSTAT, Inc., Evanston, IL, USA) version 10.0 was used for all statistical analysis. Analysis of variance (ANOVA), linear regressions and Fisher LSD mean comparison test were applied. The significance levels used was 0.05.

Results and Discussion

Physicochemical properties

Considering single and blend films, they were uniform and homogeneous with thicknesses of about 60 µm. Table 1 shows physicochemical, barrier and optical properties of films.

Film opaque values of single compounds did not differ significantly ($p>0.05$). On the other hand, the blend CMC:PVOH showed a significant effect on the opacity, which reached 37.5

Au x nm, increasing 129% in relation to PVOH opacity. Meanwhile, the blends without UV treatment did not present significant differences ($p>0.05$) between them, irrespective of the addition of SB. However, opacity increased about 21% after UV treatment compared to the blend films. The decrease in opacity meant an increase in transparency, which is desirable when the film is to be used as packaging material [36].

The transparency was significantly different between single films ($p<0.05$). PVOH film exhibited the highest transparency (the lowest transparency value). The results showed that the blend of the polymers resulted in decreasing the transparency. The value of the blend CMC:PVOH was 2.01 whereas for UV treated blend films increased significantly ($p<0.05$). The decrease in transparency could possibly arise from the higher interaction between PVOH and CMC molecules when the photosensitizer was applied. According to Nawapat et al. [37], it could be said that the presence of photosensitizer and exposing to UV light decreased the transparency of the films.

It is well known that natural polymers as cellulose derivatives are characterized by their hydrophilic character; this property produces important shortcomings in packaging applications. Therefore, CMC films exhibited the highest moisture content. The addition of PVOH, which had the lowest humidity values, to the formulation decreased the water content of blend films significantly ($p<0.05$) (Table 1). However, neither the subsequent addition of SB nor the UV treatment modified significantly the humidity of the blend ($p>0.05$). In the case of water barrier properties, CMC films presented the highest WVP values, in contrast to the lowest one for PVOH films, which were attributed to the high crystallinity of the polymer. When both polymers were mixed, the water barrier gave a value between those of single films remaining relative stable in the presence of SB with and without UV treatment.

According to McHugh et al. [38] the addition of polar additives may increase the hydrophilic character and the solubility coefficient of the film. Moreover, additives such as sorbic acid or

p-aminobenzoic acid weaken chain packing in the film to produce a looser structure, which increases water mobility [39].

Taking oxygen permeability into account, similar trend was observed as can be seen in Table 1, except in the case of CMC:PVOH/SB which exhibited higher values compare to both, blend CMC:PVOH and matrix treated with UV.

CMC and PVOH films were immersed in water at room temperature causing their dissolution in a large extension, losing their structural characteristics. In the same way, blend films were completely solubilized. Therefore, in all these cases the determination of the swelling was not possible.

However, the sensitized irradiated films were rendered partially insoluble in water in which they were originally soluble, maintaining their structural integrity. In this case, solubility and swelling were 57%±2 and 442%±21. Similar behavior was informed by Detduangchan and Wittaya [19]. Delville et al. [40] also showed that a network structure formation occurred during the UV irradiation of wheat starch films using sodium benzoate as a photosensitizer.

Mechanical properties

Tensile is an important property that defines the capacity of film resistance to rupture when films are subjected to forces [41]. The stress–strain curves showed the mechanical responses of the films (Figure 1). Figure 1a depicts the non-lineal model (Eq. 3) used to estimate the elastic modulus which fitted the experimental data satisfactorily (data shown in table insert in Figure 1) with $r^2>0.99$.

As shown in Figure 1a, the stress (σ_v) of CMC, PVOH and their blends exhibited the highest values ($p>0.05$). Although, blend films containing SB with and without UV treatment showed lower values, they did not show significant differences ($p> 0.05$). In formulations with SB the strain (ε_v) of the blends was improved compare to CMC:PVOH films. It to be noticed that the

effect on elongation could be related with the interactions developed between the polymers and the active compound. In the same way, Sayanjali et al. [42] reported that the addition of potassium sorbate as an antimicrobial component in carboxymethyl cellulose matrices reduces the linkages of polymer structure. However, the addition of SB and subsequent exposure to UV radiation decreased again the strain values of blends showing, nevertheless, the same patterns of stress-strain.

Figure 1b shows the mechanical patterns of assays performed on a texture analyzer. The obtained results were similar to those evaluated by uniaxial tension tests.

CMC films exhibited a behavior of a stiff and brittle material, while PVOH matrix presented a pattern corresponding to a flexible film with a strain of 130%. Blend films did not show an intermediate behavior that reflex the weighted contribution of each polymer, revealing a nearest behavior to CMC matrix.

X-Ray diffraction analysis

X-Ray patterns were used to estimate the crystallinity of PVOH and CMC powders, as well as of single and blend films. For the pristine CMC powder, a broad peak was located around 2θ=21º (data not shown), indicative of an amorphous structure. The pristine PVOH powder presented the characteristic peaks at 2θ = 11.3, 19.4, 22.4 and 40.4º, in accordance with the values informed in literature [43, 44, 11, 12].

Typical XRD patterns of PVOH and CMC films and their blend with and without UV treatment are represented in Figure 2. The XRD spectrum of CMC film exhibited a peak at 2θ = 21º and a CD about 8%, whereas the spectrum of PVOH showed a sharp crystal diffraction peak at 2θ = 19.7º and a CD of 30.7% (Figure 2 and Table insert). Lin et al. [45] found that when the degree of substitution of CMC is higher than 1.0 the crystalline peaks almost disappear. Also, it has been reported that CMC has a crystallinity of about 8% [46]. The

diffraction peak at 2θ = 19 ° decreases with the degree of substitution (DS) due to the rate of alkylation of cellulose by chloroacetic acid. The diffraction peaks of CMC:PVOH were located at 2θ = 19.7 and 10.7º, being its crystallinity degree of 22.5%. According to Zhang et al. [14], this result indicates that a new structure is formed, as a consequence of hydrogen bonds between –OH and –COONa of CMC and –OH of PVOH molecules.

There was a perceptible change in the peak intensity of blend films in comparison with the pristine polymers. Observed changes can be explained by considering that for semi-crystalline amorphous blends, the noncrystallizing component could strongly modify the crystallization behavior of crystallizing component [5].

In the presence of SB did not observe changes in the diffraction pattern as well as after the treatment with UV light, except for the disappearing of the peak located at 10.7º. The results suggested that the crosslinking reaction decreased the crystallinity of films. Similar tends were informed by Detduangchan and Wittaya [19] working with starch matrices with SB as a photosensitiser treated con UV. Fama et al. [47] found that tapioca starch film without potassium sorbate (PS) had 36% crystallinity whereas film with 6% PS had 12% crystallinity, indicating an interaction of active compound with tapioca starch.

Thermal properties

The MDSC thermograms of CMC, PVOH and their blend are shown in Figure 3.

Transition temperatures and melting enthalpy values (ΔH, J g^{-1}) associated with each endothermic event obtained through the analyses of MDSC curves for single polymer samples and blend films with and without treatment are summarized in Table 2.

In CMC films, an endothermic peak located at 124ºC attributed to the loss of residual moisture was observed (Figure 3). Similar results were informed by Li et al. [48].

On the other hand, PVOH thermogram displayed two endothermic events. The first peak was the result of a thermal effect corresponding to the moisture evaporation from the sample and the second endothermic transition at 207ºC was attributed to the melting of the crystalline phase. In this case, the crystallinity degree (CD) of PVOH was estimated from Eq. (4), obtaining a value similar to that found by X-ray measurement (Figures 2, 3 and Table 2). This result was in accordance with that reported by Hasimi et al. [30] for PVOH films prepared using a polyvinyl alcohol of 89% hydrolysis.

Blend films showed two endothermic events; the enthalpy of the first peak increased regarding to PVOH matrix due to the higher moisture content attributed to the addition of CMC (Table 1). Meanwhile the entalphy of the endothermic peak corresponding to the melting of the crystalline phase became less prominent, with a 20% reduction (Figure 3 and Table 2). These results were in correspondence with the decrease of CD.

The decrease in heat of melting suggested that the crystallinity and perfection of the crystal structure were reduced in blend matrices [5]. A change in the crystalline structure may result from polymer-polymer interactions in the amorphous phase; therefore, disorder in the crystals was created, reducing the enthalpy of the phase change (Table 2). Similar behavior was observed in blend films with SB untreated and photo-crosslinked by using UV radiation. Nishio and Manley [49], working with blends of cellulose and PVOH, also found that the depression of the melting temperature suggests some kind of interaction between the two polymers.

In the presence of SB, the characteristics of the amorphous phase of the matrix prevailed while the crystallinity degree values experienced a decreased (Table 2). These results were supported by X-rays (Figure 2). After the UV treatment there was a rearrangement of the structure of the polymer chain in the network with a significant shift ($p<0.05$) of both endothermic events to lower temperatures. Only the amorphous region is expected to be

accessible to chemicals and free radical attack. The changes involved the thickness of the crystallites and the degree of crystallinity [22]. The chemical changes as a result of the photo-crosslinking due to the UV treatment affected the matrix morphology.

Dynamic mechanical analysis (DMA)

When CMC and PVOH films were scanned by DMA, two relaxations β and α were found in order of increasing temperatures (Figure 4). The β relaxations of CMC and PVOH were located around -20 ºC and -50 ºC, respectively. Krumova et al. [43] considered this relaxation in hydrophilic materials as a typical water relaxation, as a consequence of hydroxyl motions favored by the water molecules. The temperature location of the maximum of the β relaxation was attenuated in the presence of SB and even more after the UV treatment. In addition, the intensity of this relaxation decreased. These changes could be explained because of the slight restriction of the side chain movements due to the presence of SB or the density increase owing to the crosslinking in irradiated samples.

The second peak in tan δ curves of dynamic mechanical spectra of CMC and PVOH films corresponded to the α relaxation. The temperature at which it took place can be labeled as dynamic glass transition temperature (T_g).

A single composition-dependent glass-transition temperature is indicative of blend miscibility. The observation of two separate T_g supports an partially miscible system. The appearance of two relaxation transitions is the first sign of the heterogeneous two-phase structure materials [50]. Although it is possible to distinguish a phase separated system from a miscible one by DSC if the T_gs of the components are more than 20°C apart [51], in the present study it was not achieved except by DMA technique. DMA curves of CMC:PVHO films revealed two main thermal events at increasing temperatures, which closely matched the

glass transitions of PVOH-enriched phase and CMC-enriched phase, respectively (Figure 4 and Table insert).

In order to explain these behavior, the complexity of the study system has to take in account. According to Krumova et al. [43], it is known that PVOH is a semicrystalline polymer in which physical interactions between the polymer chains are due to hydrogen bonding between the hydroxyl groups. Thereby the introduction of SB as well as the crosslinking with UV radiation affected both, crystallinity and physical network, originating variations in the T_g values of the system. The shift of the blend T_gs would be a sign of a partial miscibility between the homopolymers due to polymer-polymer interactions. Furthermore, the shift of transition temperatures along the temperature scale is a sign of incomplete phase separation as well as of the appearance of an interphase (cita). The T_gs of CMC-enriched phase underwent a shift toward higher temperatures ($p<0.05$) while the T_gs of PVOH-enriched phase were found at lower temperatures ($p<0.05$), in relation to their corresponding single films. This percentage of change was more marked in this latter case, inferring that the modification of the matrix composition because of the addition of SB or UV treatment would have higher effect on the PVOH-enriched phase.

Fourier transform infrared spectroscopy

As UV light provides a lower energy level than other source of ionizing radiation, it is impossible for direct cleavage of C-C or C-H bond occur for the formation of free radicals. Hence, for crosslinking purposes, there is need for a photosensitizer (photo initiator) that can absorb a low-energy photon (UV light) and become activated. This leads to the formation of free radicals and also leads to macro radical combination by hydrogen abstraction [40].

The mechanism of crosslinking is not completely elucidated at present. However, according to Miranda et al. [52], it is probable that a free radical arising from the photolysis of sodium

benzoate would abstract a tertiary hydrogen atom from the polymer chain to yield a polymeric radical, which can crosslink by combination with another such radical.

Figure 5a shows the infrared spectra of CMC (a) and PVOH (b) in the range 3800–800 cm^{-1}. Both polymers possess some similar functional groups, therefore the group regions of IR spectra are partially the same and their spectra differ mainly in the fingerprint regions. The spectra of blend films showed peaks characteristic of both components.

The PVOH spectrum showed a characteristic band in the 3700-3000 cm^{-1} region, which indicated the presence of a broad range of associated hydroxyls. The stretching band at 1141 cm^{-1} is known to be a crystallization-sensitive band of PVOH and is taken as a measure of the degree of crystallinity [6, 14, 53]. It was mitigated by the presence of SB and even more when films were exposed to UV radiation. These findings supported the aforementioned reductions of crystallinity degree obtained by using DSC and X-ray techniques.

In CMC spectrum the band in the area of 3385 cm^{-1} was the result of hydrogen-bonded OH stretching vibration while the peak at 2939 cm^{-1} was attributed to the CH stretching vibration in cellulose and hemicelluloses [13].

The FTIR spectra of CMC:PVOH displayed an absorption band at 3353 cm^{-1} due to the OH stretching vibrations of CMC and PVOH. As can be seen in Figure 5b, additional bands at 1020–900 cm^{-1} due to CH stretch appeared. The band at 1595 cm^{-1} was attributed to the characteristic absorptions of asymmetrical stretching vibration of carboxylate anion (COO^{-}) of CMC. The FTIR spectra of blend SB unirradiated and irradiated are also shown in Figure 5b. They showed that the absorption intensities at 1558 cm^{-1} characteristic of the CMC:PVOH/SB disappeared when films were exposed to UV light, indicating that the sensitizer was photo-decomposed whereas the peak at 1379 cm^{-1} decreased and exhibited a shift to 1386 cm^{-1} once exposed to irradiation. These findings are in accordance with those found by Miranda et al. [52], working on crosslinking of PVOH by UV in the presence of SB.

Due to the low amount of SB used in the current work and with the purpose of clarifying the interaction between the compounds, higher SB concentrations were added, ranging from 0.1 to 1.

Clear evidence for the successful attachment of some active groups on the film surface was obtained with a higher SB amount. As can be visualized in Figure 5c the band at 1420 cm^{-1} of blend film with 0.1% SB shifted to 1406 cm^{-1} with the addition of 0.5% SB. Meanwhile, the peak of 1379 cm^{-1} underwent a displacement to 1390 cm^{-1}. The band at 1327 cm^{-1} decreased and the shoulder at 1558 cm^{-1} became into a sharp peak with increasing SB concentrations. After it was exposed to radiation, this latter peak did not disappear but dramatically decreased its intensity whereas the band a 1379 cm^{-1} disappeared. Bands at 846, 725 and 680 cm^{-1} also sharpened with higher SB concentrations, but they underwent intensity attenuations after UV treatment.

Microstructure

Visually, the two polymers appear to be well mixed in the film matrices and there seems to be no distinct phase separation. From the microscopic point of view, in cross section, single films had a homogeneous appearance, with good structural integrity, without pores. Meanwhile, in blend films, both polymer materials were observed as interspersed layers, forming a network of granular appearance (Figure 6a), with co-continuous domains, which could support the aforementioned phases, one CMC-enriched and the other PVOH-enriched phase. This lack of homogeneity became more pronounced in the presence of SB. As can be observed in Figure 6b, clear domains and dark regions were observed possibly due to the change in the degree of crystallinity as could be observed by X -ray. When blend films with the addition of SB underwent the treatment with UV light, structural changes occurred, presenting an appearance of a lattice like a honeycomb (Figure 6c). The microscopic images

revealed that the surface morphology of the single and CMC:PVOH films with and without the addition of SB was soft. In contrast, blend films undergoing UV radiation presented rougher surfaces compared to those without treatment.

Antimicrobial capacity

The effectiveness of use of preservatives is often dictated by the sensitivity of the microorganisms themselves. *E. coli* and *Salmonella* spp. has been associated with serious food contamination and poisoning. On the other hand, it was expected that the predominant microorganisms were fungi and yeasts. Therefore *Penicillium* spp. and *Candida* spp. were used to complete the evaluation of the antimicrobial properties of films bearing in mind potential applications to food matrices.

Figure 7 shows the results of the antimicrobial test performed on CMC-PVOH blends and films containing SB with and without UV treatment. The percentage and diameter of inhibition area against *Penicillium* spp., *Salmonella* spp., *E. coli* and *Candida* spp. are shown in Table 3.

In all cases, the most diluted concentration of inoculum allowed a better visualization of the film inhibitory effect. Figure 7 shows the agar plate containing control films and matrices CMC:PVOH/SB with and without UV treatment for all microorganisms assayed. As expected, the control sample did not inhibit microbial growth. Films containing SB inhibited the microbial growth by contact with the culture medium, irrespective of the microorganism tested. Stanojevic et al. [54] described the strongest antifungal activity manifested by sodium benzoate against the species *Candida* spp. and *Penicillium* spp. Irradiated samples also showed inhibition halo. Although, the antimicrobial capacity of films decreased with UV treatment, the matrices retained their antimicrobial character. Concerning CMC:PVOH/SB films, it can be inferred that the UV treatment reduced by 22, 40 and 47% the percentage of inhibition for *Salmonella* spp., *E. coli* and *Penicillium* spp., respectively.

In the case of *Candida* spp. (Figure 7b) the inhibition was complete after 24 h of incubation. As can be seen in Figure 7 the films containing SB maintained their antimicrobial capacity after the UV treatment.

Conclusions

The new materials obtained presented different thermal and chemical stability than those of single components. Taking into account the obtained results of the blend films as well as films treated with UV radiation, oxygen barrier properties showed a very low value even in comparison with synthetic films, which would allow their application as packaging with selective oxygen permeability.

Thermal analysis, X-Ray, SEM and FT-IR evidenced the microstructural changes occurred in the matrix, which provided supplementary information about the modification induced either by the presence of sodium benzoate or UV treatment.

FT-IR spectra reflected some degree of interaction polymer-polymer at a molecular level in the amorphous regions, especially in blend films photo-crosslinked in the presence of SB. The formation of carbonyl groups occurred to some extent during the radiation process, proving that the ultraviolet method was successfully applied.

The incorporation of sodium benzoate combined with UV treatment in blend films was positive from the microbial point of view because of the growth inhibition of a wide spectrum of microorganisms. Meanwhile from a physicochemical perspective the treatment of the blends/SB with UV radiation also changed their morphology rendering them more insoluble in water, turning the functionalized blend films into a potential material to be applied as food packaging.

Rerefences

[1] L.Weng, L.Zhang, D.Ruan, L.Shi, J.Xu J, Thermal gelation of cellulose in a NaOH/thiourea aqueous solution, Langmuir 20 (2004) 2086-2093.

[2] K. Guo, C.C. Chu, Synthesis and characterization of novel biodegradable unsaturated poly(ester amide)/poly(ethylene glycol) diacrylate hydrogels, J. Polym. Sci. Part A: Polym. Chem. 43 (2005) 3932-3944.

[3] J. Deng, Q. He, Z. Wu, W. Yang, Using glycidyl methacrylate as cross-linking agent to prepare thermosensitive hydrogels by a novel one-step method, J. Polym. Sci. Part A: Polym. Chem. 46 (2008) 2193-2201.

[4] A.M. Bochek, I.L. Shevchuk, L.M. Kalyuzhnaya, Properties of aqueous solutions of blends of polyvinyl alcohol with carboxymethyl cellulose ionized to various extents, Russ. J. App. Chem. 83 (4) (2010) 712−717.

[5] O.W. Guirguis, M.T.H. Moselhey, Thermal and structural studies of poly(vinyl alcohol) and hydroxypropyl cellulose blends, Nat. Sci. 4 (1) (2012) 57-67.

[6] S.Kubo, J.F. Kadla, The formation of strong intermolecular interactions in immiscible blends of poly(vinyl alcohol) (PVA) and lignin, Biomacromolecules 4 (2003) 561-567.

[7] J-S. Park, J-W. Park, E. Ruckenstein, Thermal and dynamic mechanical analysis of PVA/MC blend hydrogels, Polymer 42 (2001) 4271–4280.

[8] G. Buhus, M. Popa, C. Peptu, J. Desbrieres, Hydrogels based on carboxymethylcellulose and poly (vinyl alcohol) for controlled loading and release of chloramphenicol, J. Optoelectron. Adv. Mat. 9 (2007) 3445 – 3453.

[9] X. Congming, G. Yongkang G, Preparation and properties of physically crosslinked sodium carboxymethylcellulose/poly(vinyl alcohol) complex hydrogels, J. Appl. Polym. Sci. 107 (2008) 1568–1572.

[10] M.F. Abou Taleb, H.L. Abd El-Mohdy, H.A. Abd El-Rehim, Radiation reparation of PVA/CMC copolymers and their application in removal of dyes. J. Hazard. Mat. 168 (2009) 68–75.

[11] C.V. Prasad, H. Sudhakar, B.Y. Swamy, G.V. Reddy, C.L.N. Reddy, S. Suryanarayana, M.N. Prabhakar, M.C.S Subha, K.C. Rao, Miscibility studies of sodium carboxymethylcellulose/ poly(vinyl alcohol) blend membranes for pervaporation dehydration of isopropyl alcohol, J. Appl. Polym. Sci. 120 (2011) 2271–2281.

[12] X. Cai, Q. Zhao, Y. Luan, Y. Jiang, J. Shi, W. Shao, Polymer fibrous materials composed of sodium carboxymethylcellulose and poly(vinyl alcohol) for a hydrophilic anticancer drug release, J. Disper. Sci. Technol. 33 (2012) 835–839.

[13] M.M. Ibrahim, A. Koschella, G. Kadry, T. Heinze, Evaluation of cellulose and carboxymethyl cellulose/poly(vinyl alcohol) membranes, Carbohyd. Polym. 95 (2013) 414–420.

[14] L. Zhang, G. Zhang, J. Lu, H. Liang, Preparation and characterization of carboxymethyl cellulose/polyvinyl alcohol blend film as a potential coating material, Polym. Plast. Tech. Eng. 52 (2013) 163–167.

[15] J.P. Foussier, J.F. Rabek. (Vol. Eds.) (1993). Radiation curing in polymer science and technology: Vol. 1.5. London: Elsevier.

[16] R. Bhat, A.A. Karim, Impact of radiation processing on starch, Compr. Rev. Food Sci. Food Safety 8 (2) (2009) 44-58.

[17] M.A. Khan, S.K. Bhattacharia, M.A. Kade, K. Bahari, Preparation and characterization of ultra violet (UV) radiation cured bio-degradable films of sago starch/PVA blend, Carbohyd. Polym. 63 (2006) 500–506.

[18] A. Sionkowska, A. P1anecka, J. Koz1owska, J. Skopińska-Wiśniewska, Photochemical stability of poly(vinyl alcohol) in the presence of collagen, Polym. Degrad. Stabil. 94 (2009) 383–388.

[19] N. Detduangchan, T. Wittaya, Effect of UV-treatment on properties of biodegradable film from rice starch, World Academy Sci. Eng. Tech. 57 (2011) 464-469.

[20] K. Chen, Y. Lin, Immobilization of microorganisms with phosphorylated polyvinyl alcohol (PVA) gel. Enzyme. Microb. Technol. 16 (1994) 79-83.

[21] K. Takakura, G. Takayama, J. Ukida, Ultraviolet-induced crosslinking of poly(vinylalcohol) in the presence of sensitizers, Appl. Polym. Sci. J. 9 (1965) 3217-3224.

[22] P. Ghosh, R. Gangopadhay, Photo functionalisation of cellulose and lignocelluloses fibres using photoactive organic acids, Eur. Polym. 36 (3) (2000) 625-634.

[23] S.K. Sagoo, R. Board, S. Roller, Chitosan potentiates the antimicrobial action of sodium benzoate on spoilage yeasts, Lett. Appl. Microbiol. 34 (3) (2002) 168–172.

[24] S. Villarruel, S. Rivero, A. Pinotti, Propiedades térmicas y estructurales de películas compuestas de poli (vinil alcohol) y carboximetilcelulosa, IV Congreso Internacional de Ciencia y Tecnología de los Alimentos, Córdoba, Argentina, November 2012.

[25] Argentine Food Code (2004). Capítulo XII. http://www.anmat.gov.ar/alimentos/codigoa/Capitulo_XII.pdf. Buenos Aires: De la Canal y Asociado.

[26] S. Cho, Ch. Rhee, Mechanical properties and water vapor permeability of edible films made from fractionated soy proteins with ultrafiltration, LWT 37 (2004) 833–839.

[27] Y. Zhang, J.H. Han, Plasticization of Pea starch films with monosaccharides and polyols, J. Food Sci. 71 (2006) 253-261.

[28] ASTM (1995). Standard test methods for water vapor transmission of material, E96- 95. In Annual book of ASTM. Philadelphia, PA: American Society for Testing and Materials.

[29] S. Rivero, M.A. García, A. Pinotti A, Crosslinking capacity of tannic acid in plasticized chitosan films, Carbohyd. Polym. 82 (2010) 270–276.

[30] A. Hasimi, K.G. Stavropoulou, M. Papadokostaki, Sanopoulou, Transport of water in polyvinyl alcohol films: Effect of thermal treatment and chemical crosslinking, Eur. Polym. J. 44 (2008) 4098-4107.

[31] N.A. El-Zaher, W.G. Osiris, Thermal and structural properties of poly(vinyl alcohol) doped with hydroxypropyl cellulose, J. Appl. Polym. Sci. 96 (2005) 1914–1923.

[32] M.C. Galdeano, M.V.E. Grossmann, S. Mali, L.A. Bello-Perez, M.A. Garcia, P.B. Zamudio-Flores, Effects of production process and plasticizers on stability of films and sheets of oat starch, Mat. Sci. Eng. C 29 (2009) 492–498.

[33] J. Piermaria, A. Pinotti, M.A. Garcia, A. Abraham, Films based on kefiran, an exopolysaccharide obtained from kefir grain: Development and characterization, Food Hydrocolloid. 23 (2009) 684-690.

[34] M. Molina, L. Giannuzzi, Combined effect of temperature and propionic acid concentration on the growth of Aspergillus parasiticus, Food Res. Inter. 6 (1999) 677-682.

[35] S. Rivero, L. Giannuzzi, M.A. García, A. Pinotti, Controlled delivery of propionic acid from chitosan films for pastry dough conservation, J. Food Eng. 116 (2013) 524–531.

[36] C.H. Chen, W.S. Kuo, L.S. Lai, Rheological and physical characterization of forming solutions and edible films from tapioca starch/decolorized hsian-tsao leaf gum, Food Hydrocolloid. 23 (2009) 2132-2140.

[37] D. Nawapat, W. Thawien, Effect of UV-treatment on the properties of biodegradable rice starch films, Int. Food Res. J. 20(3) (2013) 1313-1322.

[38] T. H McHugh, R. Avena-Bustillos, J.M Krochta, Hydrophilic edible films: modified procedure for water vapor permeability and explanation of thickness effects, J. Food Sci. 58 (1993) 899-903.

[39] A. Cagri, Z. Ustunol, E.T. Ryser, Properties of low pH whey protein-based edible films containing p-aminobenzoic or sorbic acids, J. Food Sci. 66(6) (2001) 865-870.

[40] J. Delville, C Joly, P Dole, C Bliard, Solid state photocrosslinked starch based films: a new family of homogeneous modified starches, Carbohyd. Polym. 49 (1) (2002) 71–81.

[41] F. Yamashita, A. Nakagawa, G.F. Veiga, S. Mali, M.V.E. Grossmann, Biodegradable active packaging for minimally processed fruits and vegetables, Brazilian J. Food Tech. 8 (2012) 335–343.

[42] S. Sayanjali, B. Ghanbarzadeh, S. Ghiassifar, Evaluation of antimicrobial and physical properties of edible film based on carboxymethyl cellulose containing potassium sorbate on some mycotoxigenic Aspergillus species in fresh pistachios, LWT 44 (2011) 1133–1138.

[43] M. Krumova, D. López, R. Benavente, M. Mijangos, J.M. Pereña, Effect of crosslinking on the mechanical and thermal properties of poly(vinyl alcohol), Polymer 41 (2000) 9265–9272.

[44] C. Xiao, Y. Gao, Preparation and properties of physically crosslinked sodium carboxymethylcellulose/poly(vinyl alcohol) complex hydrogels, J. Appl. Polym. Sci. 107 (2008) 1568–1572.

[45] X. Lin, T. Qu, S. Qi, Kinetics of the carboxymethylation of cellulose in the isopropyl alcohol system, Acta Polym. 41(1990) 220- 222.

[46] M. P. Adinugraha, D. W. Marseno, M. Haryadi, Synthesis and characterization of sodium carboxymethylcellulose from cavendish banana pseudo stem (Musa cavendishii LAMBERT) Carbohyd. Polym. 62 (2005) 164- 169.

[47] L. Fama, A. Rojas, S. Goyanes, L. Gerschenson, Mechanical properties of tapioca-starch edible films containing sorbates, LWT-Food Sci. Tech. 38(6) (2005) 631-639.

[48] W. Li, B. Sun, P. Wu, Study on hydrogen bonds of carboxymethyl cellulose sodium film with two-dimensional correlation infrared spectroscopy, Carbohyd. Polym.78 (2009) 454–461

[49] Y. Nishio, R. St J. Manley, Cellulose/poly(vinyl alcohol) blends prepared from solutions in N,N-dimethylacetamide-lithium chloride, Macromolecules 21 (1988) 1270-1277.

[50] Y. S. Lipatov, T. Alekseeva, Phase-Separated Interpenetrating Polymer Networks. Springer-Verlag Berlin Heidelberg (2007).

[51] O. Olabisi, L. M. Robeson, M. T. Shaw, Polymer–polymer miscibility. New York: Academic Press. (1979).

[52] T.M.R. Miranda, A.R. Gonçalves, M.T. Pessoa Amorim, Ultraviolet-induced crosslinking of poly(vinyl alcohol) evaluated by principal component analysis of FTIR spectra, Polym. Inter. 50 (2001) 1068-1072.

[53] L.T. Cuba-Chiem, L. Huynh, J. Ralston, D.A. Beattie, In situ particle film ATR FTIR spectroscopy of carboxymethyl cellulose adsorption on talc: binding Mechanism, pH effects, and adsorption kinetics, Langmuir 24 (2008) 8036-8044.

[54] D. Stanojevic, L. Comic, O. Stefanovic, S. Solujic-Sukdolak, Benzoate, sodium nitrite and potassium sorbate and their synergistic action in vitro, Bulg. J. Agric. Sci. 15 (4) (2009) 307-311.

Acknowledgments:

This work was supported by the Argentinean Agency for the Scientific and Technological Promotion (ANPCyT) (PICT/2012/0415) and the Argentinean National Research Council (CONICET) (PIP112-200801-01209). Authors acknowledge Ing.Javier Lecot and Daniel Russo for technical assistance.

FIGURE CAPTIONS

Figure 1. Tensile stress-strain behavior of films of polyvinyl alcohol (PVOH), carboxymethyl cellulose (CMC), blend film, blend with the addition of sodium benzoate (SB) exposed to UV radiation determined by a) quasi-static method and b) texture analyzer. Continuous lines indicate data fitted by Eq. 3.

Figure 2. X-ray diffractograms of PVOH and CMC films, CMC:PVOH/SB and CMC:PVOH/SB UV. Table insert shows the crystallinity degree (CD) of all formulations.

Figure 3. MDSC **t**hermograms of single films, blend films, CMC:PVOH/SB and CMC:PVOH/SB UV.

Figure 4. DMA spectra showing tan δ of PVOH and CMC films, CMC:PVOH, blend/SB with and without expose to UV treatment. Table insert shows the T_gs of CMC-enriched phase and PVOH-enriched phase.

Figure 5. FTIR spectra of: a) CMC and PVOH films, b) CMC:PVOH, CMC:PVOH/SB (0.1%) and CMC:PVOH/SB UV films and c) blend film, blend/SB 0.5% and blend/SB 0.5% exposed to UV radiation.

Figure 6. Cross section **S**EM micrographs of: (a) CMC:PVOH film, blend/SB and blend/SB exposed to UV radiation. Magnification: 50 nm between marks.

Figure 7. Antimicrobial properties of control blend films and matrices containing SB without and with UV radiation incubated at 37ºC against a) *Penicillium* sp. b) *Candida* spp. c) *E. coli*. and d) *Salmonella* spp.

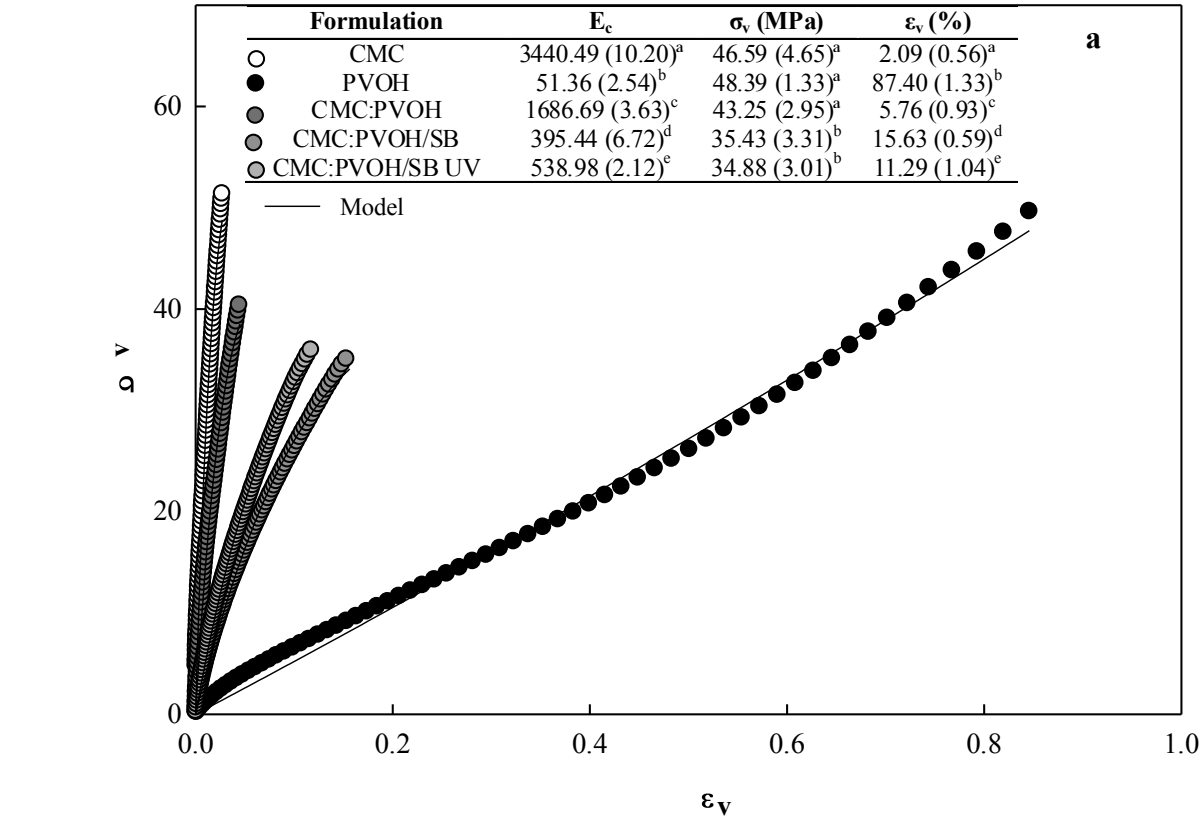
Formulation
E_c
σ_v (MPa)
ε_v (%)
CMC
3440.49 (10.20)[a]
46.59 (4.65)[a]
2.09 (0.56)[a]
PVOH
51.36 (2.54)[b]
48.39 (1.33)[a]
87.40 (1.33)[b]
CMC:PVOH
1686.69 (3.63)[c]
43.25 (2.95)[a]
5.76 (0.93)[c]
CMC:PVOH/SB
395.44 (6.72)[d]
35.43 (3.31)[b]
15.63 (0.59)[d]
CMC:PVOH/SB UV
538.98 (2.12)[e]
34.88 (3.01)[b]
11.29 (1.04)[e]
Model
a
σ v
ε_v
0
20
40
60
0.0
0.2
0.4
0.6
0.8
1.0

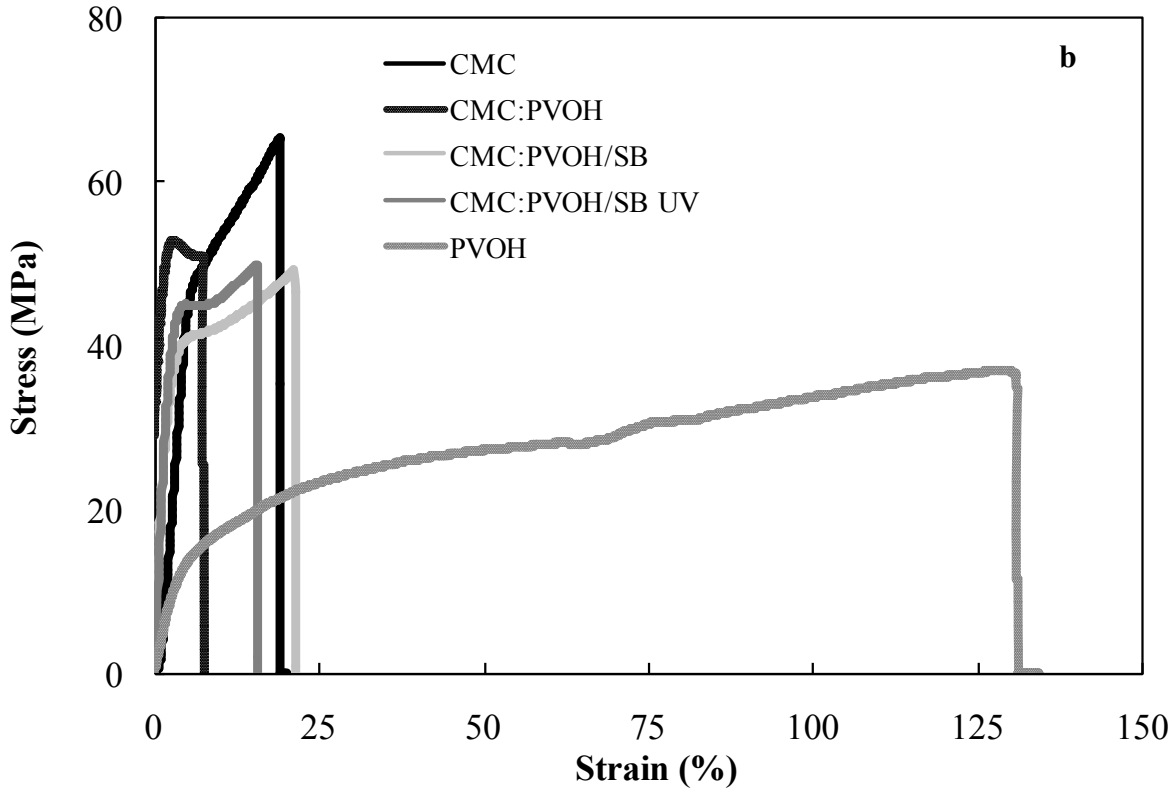
CMC
CMC:PVOH
CMC:PVOH/SB
CMC:PVOH/SB UV
PVOH
b
Stress (MPa)
Strain (%)
0
20
40
60
80
0
25
50
75
100
125
150

Figure 1

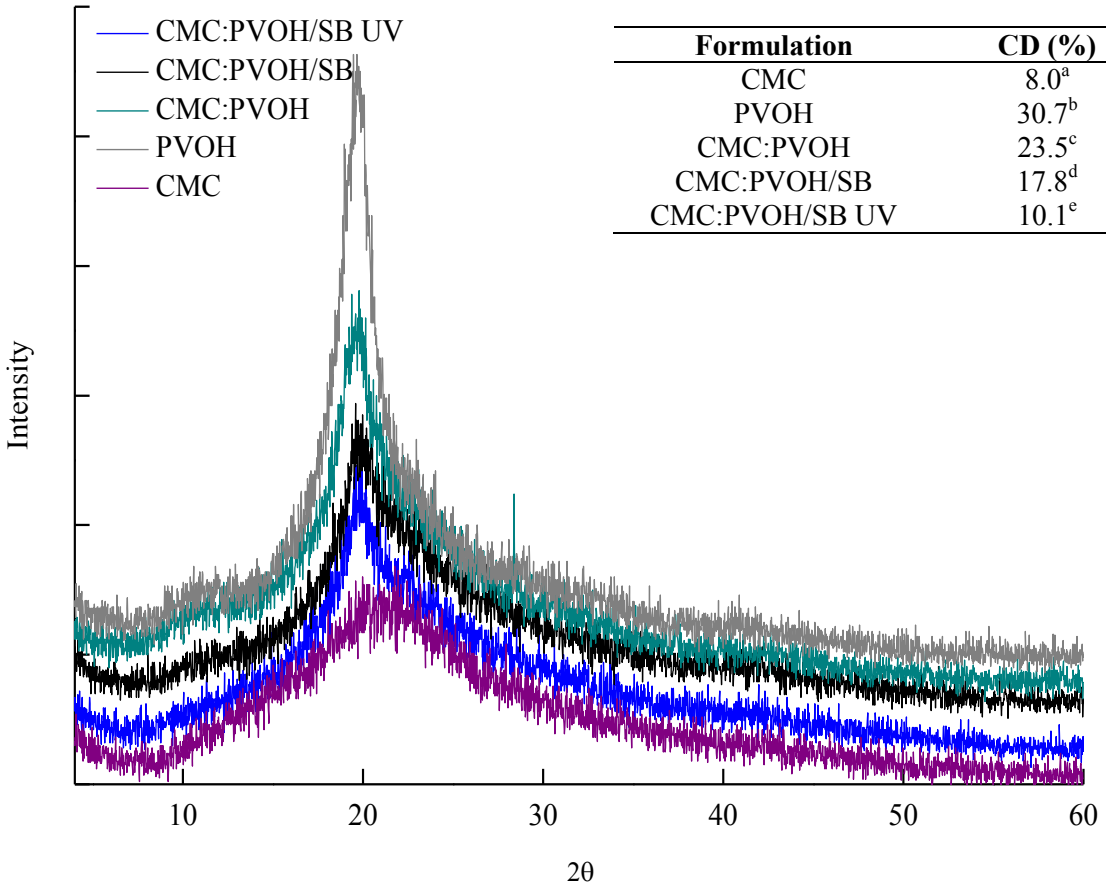

Formulation	CD (%)
CMC	8.0[a]
PVOH	30.7[b]
CMC:PVOH	23.5[c]
CMC:PVOH/SB	17.8[d]
CMC:PVOH/SB UV	10.1[e]

Figure 2

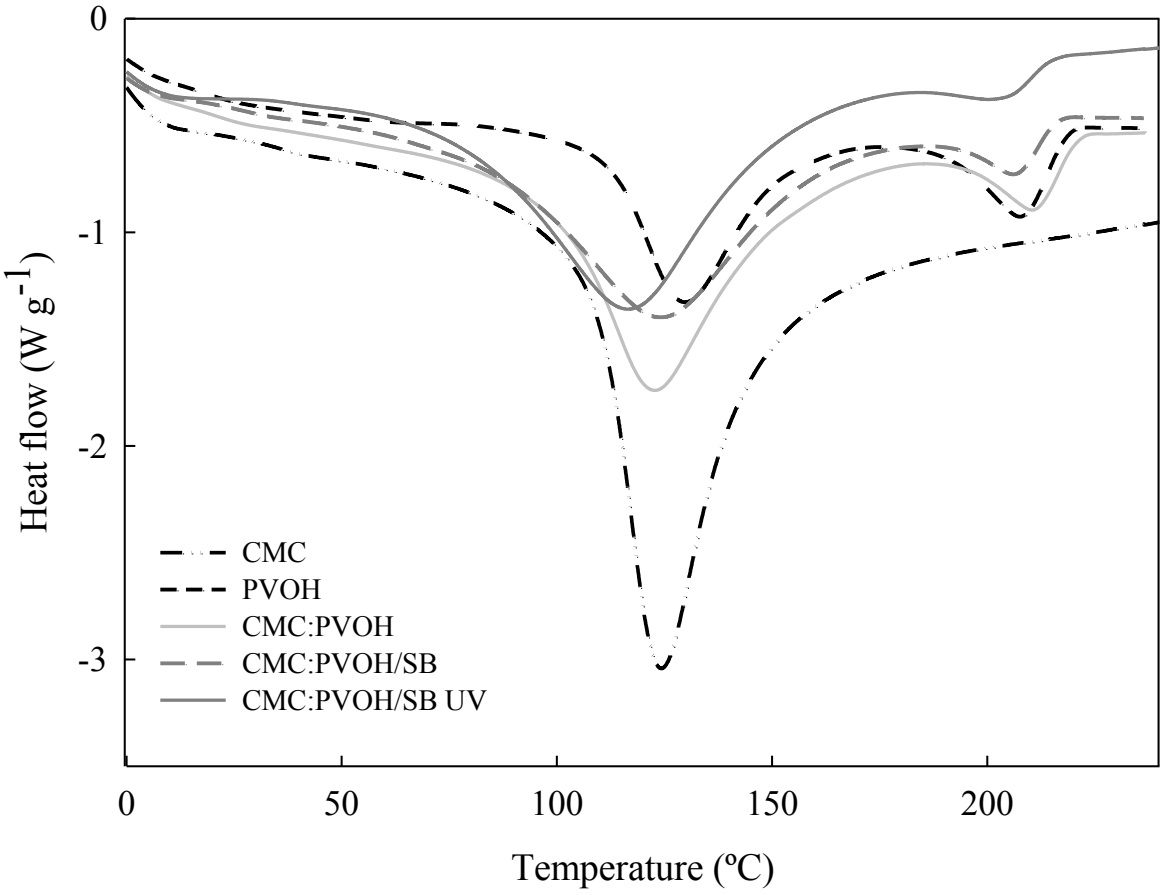
0
-1
-2
-3
Heat flow (W g-1)
0
50
100
150
200
Temperature (ºC)
CMC
PVOH
CMC:PVOH
CMC:PVOH/SB
CMC:PVOH/SB UV

Figure 3

Film	$T_{g\ PVOH\text{-}enriched\ phase}$	$T_{g\ CMC\text{-}enriched\ phase}$
CMC	--	137.8 (4.6)[a]
PVOH	55.7 (3.0)[a]	--
CMC:PVOH	43.8 (2,8)[b]	148.3 (0.8)[b]
CMC:PVOH/SB	37.2 (3.0)[c]	139.2 (2.5)[a]
CMC:PVOH/SB UV	46.5 (2.4)[b]	156.8 (2.4)[c]

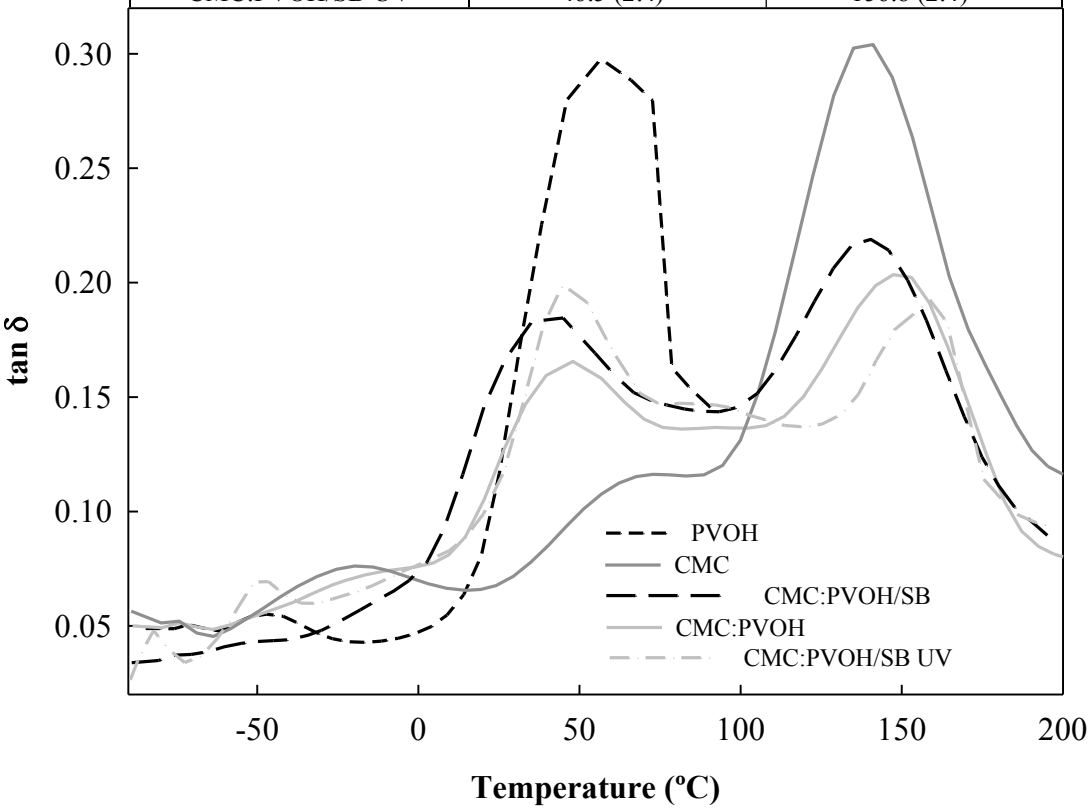

Figure 4

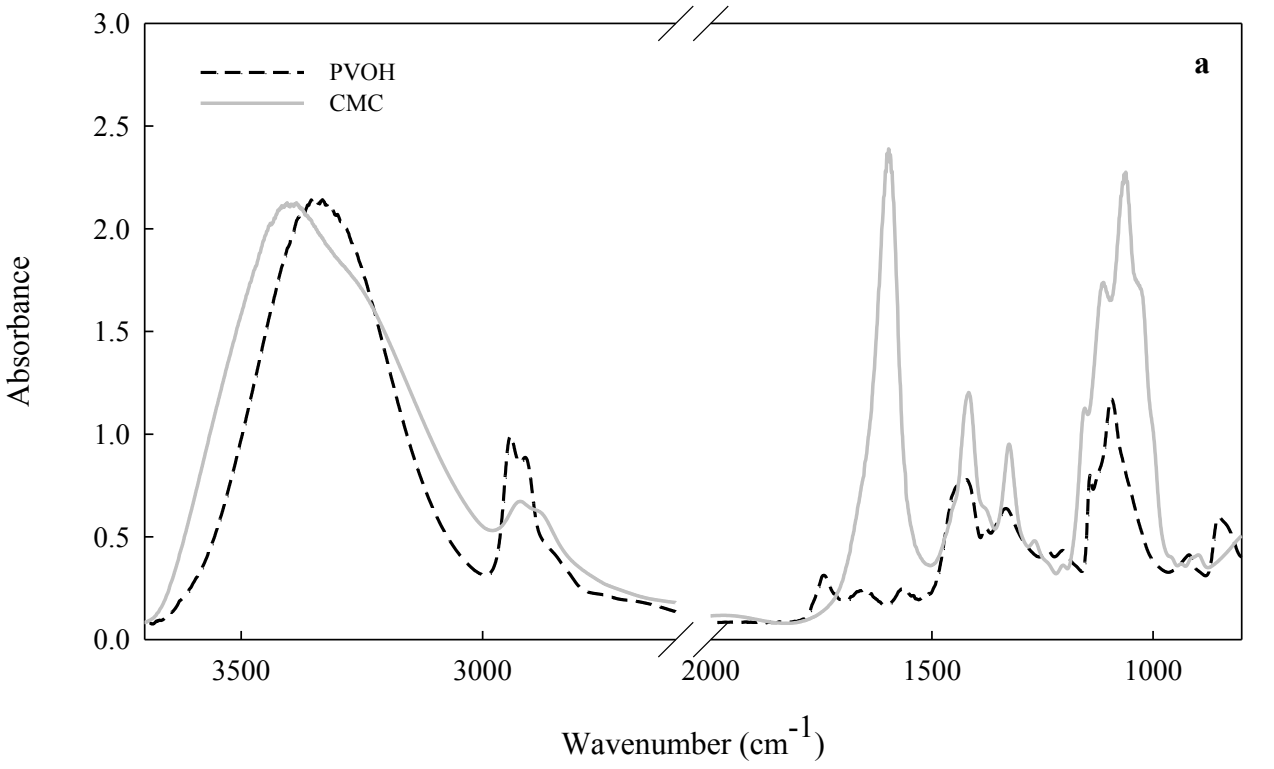
a
PVOH
CMC
Absorbance
Wavenumber (cm-1)
3.0
2.5
2.0
1.5
1.0
0.5
0.0
3500
3000
2000
1500
1000

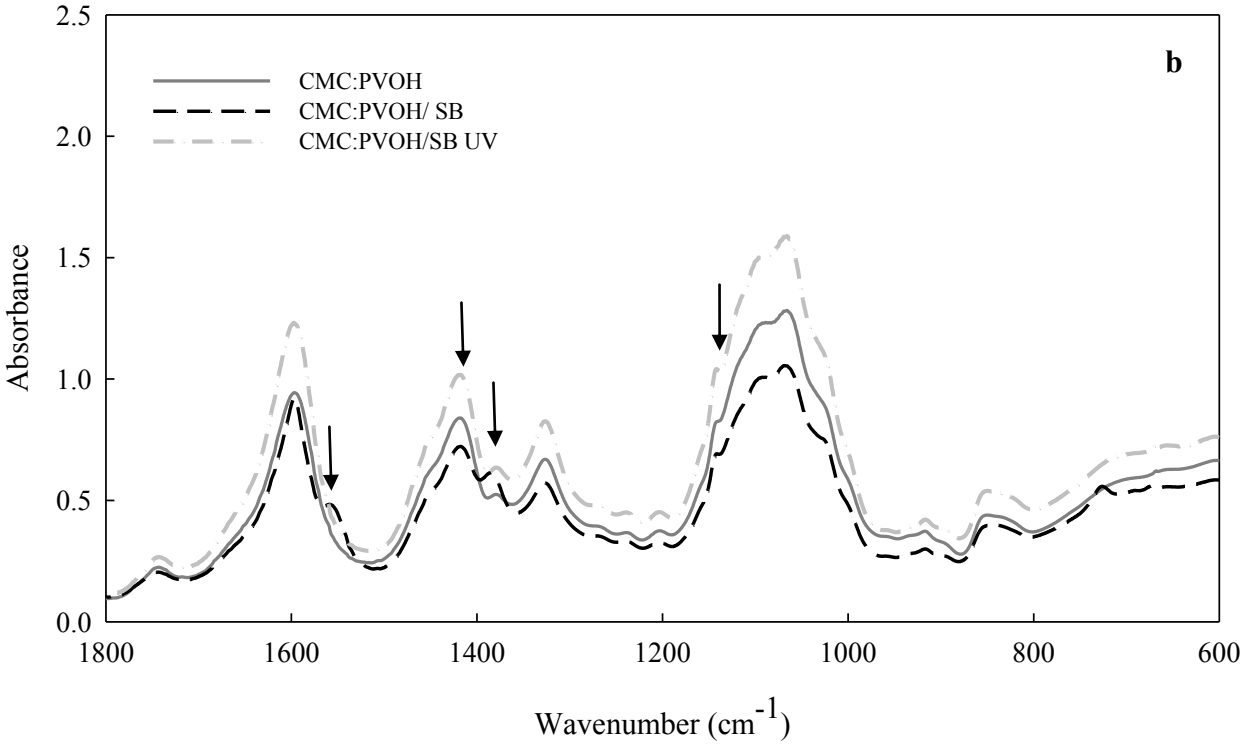
b
CMC:PVOH
CMC:PVOH/ SB
CMC:PVOH/SB UV
Absorbance
Wavenumber (cm-1)
2.5
2.0
1.5
1.0
0.5
0.0
1800
1600
1400
1200
1000
800
600

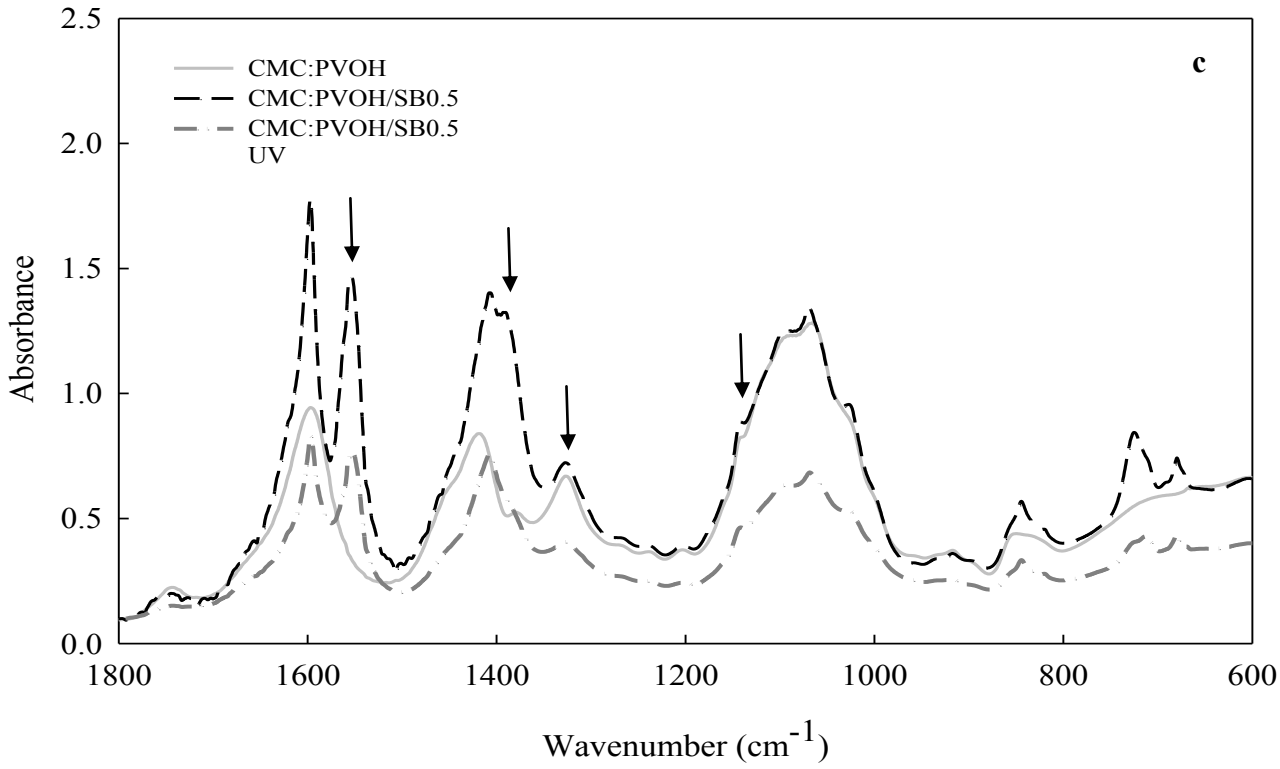
CMC:PVOH
CMC:PVOH/SB0.5
CMC:PVOH/SB0.5
UV
c
Absorbance
Wavenumber (cm-1)
2.5
2.0
1.5
1.0
0.5
0.0
1800
1600
1400
1200
1000
800
600

Figure 5

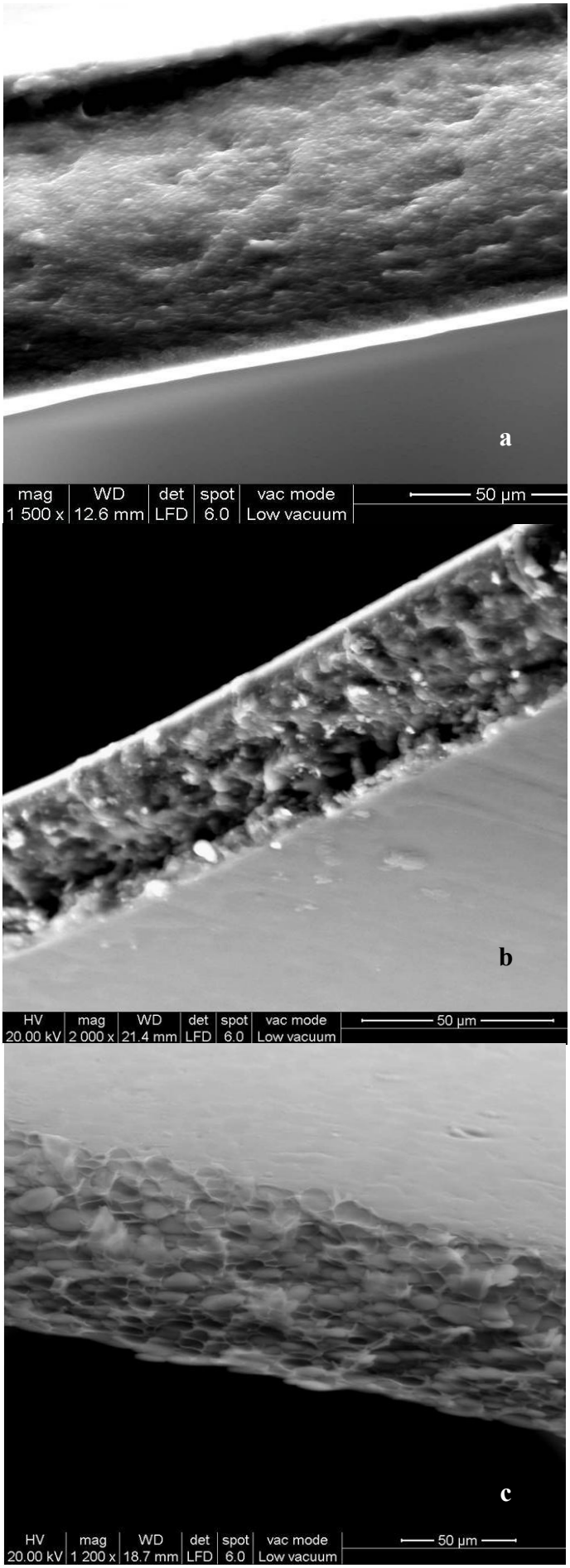
a
mag
1 500 x
WD
12.6 mm
det
LFD
spot
6.0
vac mode
Low vacuum
50 µm
b
HV
20.00 kV
mag
2 000 x
WD
21.4 mm
det
LFD
spot
6.0
vac mode
Low vacuum
50 µm
c
HV
20.00 kV
mag
1 200 x
WD
18.7 mm
det
LFD
spot
6.0
vac mode
Low vacuum
50 µm

Figure 6

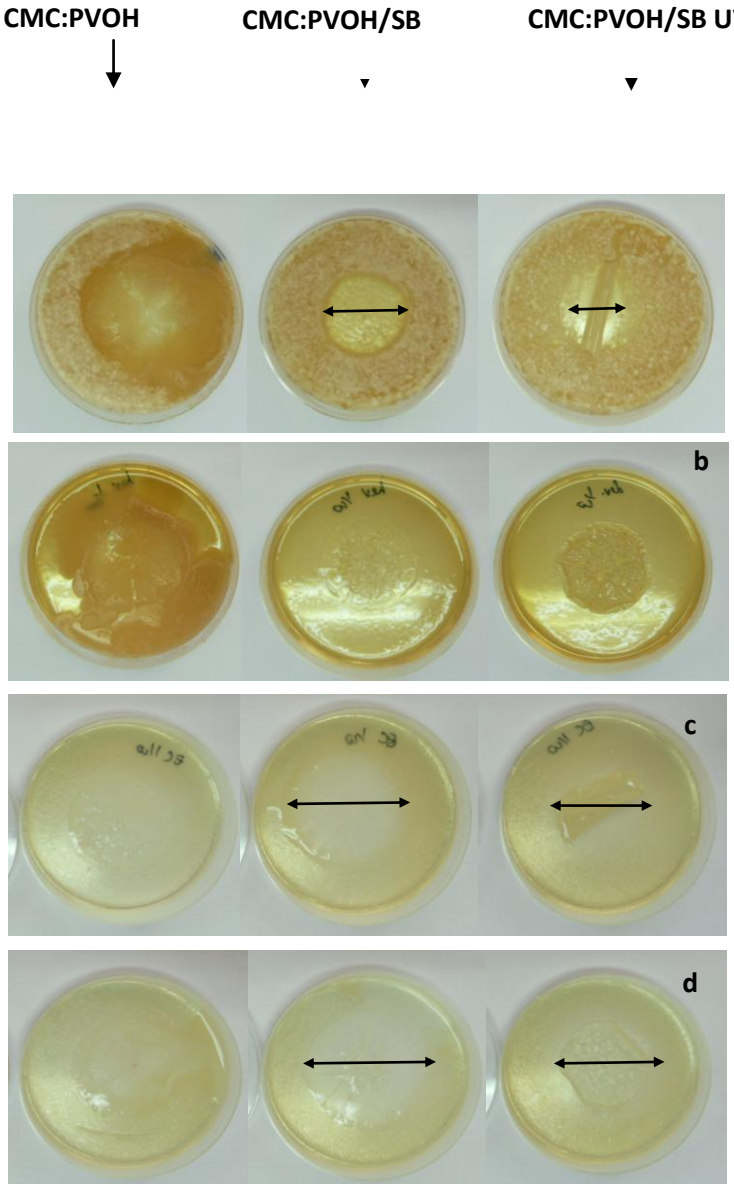

Figure 7

Table 1: Physicochemical properties of films with and without treatment

Film composition	Oxygen permeability x 10^{15} ($cm^3\ m^{-1}\ s^{-1}\ Pa^{-1}$)	WVP x 10^{11} ($g\ s^{-1}\ m^{-1}\ Pa^{-1}$)	Humidity content (%)	Optical properties	
				Film Transparency ($A_{600}\ mm^{-1}$)	Film opacity (Au **x** nm)
PVOH	2.54 (0.08)[a]	0.83 (0.39)[a]	5.24 (0.29)[a]	0.45 (0.01)[a]	16.36 (0.56)[a]
CMC	44.22 (0.22)[b]	7.68 (0.94)[b]	24.06 (0.54)[b]	1.15 (0.09)[b]	19.02 (0.93)[a]
CMC:PVOH	10.75 (0.42)[c]	2.07 (0.13)[ac]	16.08 (0.55)[b]	2.01 (0.07)[c]	37.51 (2.27)[b]
CMC:PVOH/ SB	18.64 (0.07)[d]	3.07 (0.62)[c]	15.62 (0.49)[bc]	2.07 (0.14)[c]	36.87 (2.06)[b]
CMC:PVOH/ SB UV	11.40 (0.41)[c]	2.02 (0.17)[ac]	14.89 (0.06)[c]	2.66 (0.05)[d]	46.55 (1.74)[c]

The values in parentheses correspond to the standard deviation. Different letters in the same column indicate significant differences ($p < 0.05$) between samples.

Table 2. Transition temperatures and associated events for pristine, composite films and composite films exposed to UV radiation

Film composition	Event associated to water remotion		Event associated to crystalline phase melting			
	T_p (ºC)	ΔH (J g^{-1})	T_m (ºC)	ΔH (J g^{-1})	CD (%)	% change of ΔH*
CMC	127.5 (2.15)[a]	471.7 (13.40)[a]	n d	n d	nd	nd
PVOH	154.0 (1.56)[b]	35.6 (1.68)[b]	207.7 (0.19)[a]	37.62 (4.41)[a]	27.1[a]	-0.73
CMC:PVOH	124.5 (2.64)[a]	298.5 (2.60)[c]	210.8 (0.20)[b]	29.90 (0.64)[b]	21.5[b]	-0.78
CMC:PVOH/ SB	125.7 (2.05)[a]	294.9 (5.66)[c]	206.6 (0.27)[a]	18.50 (1.45)[c]	13.3[c]	-0.87
CMC:PVOH/ SB UV	115.2 (2.11)[c]	297.7 (0.71)[c]	204.1 (0.21)[c]	13.33 (0.16)[d]	9.6[d]	-0.90

n d: no detectable

The values in parentheses correspond to the standard deviation. Different letters in the same column indicate significant differences ($p < 0.05$) between samples.

$$^{*}\%\, change \;\; of\; \Delta H = \frac{\Delta H_{m\ blended\ \ PVOH} - (\Delta H)_{pure\ PVOH}}{(\Delta H)_{\ pure\ PVOH}} \times 100$$

Table 3. Antimicrobial properties of films containing SB with and without UV treatment against inoculation of *Salmonella* spp*., S aureus, Candida* spp*.* and *Penicillium* spp*.*

Microorganism		**Observations at 24 h**		
		Inhibitory zone* (cm)	Contact**	Inhibition %
Salmonella spp*.*	CMC:PVOH	0.00 (0.00)	-	0
	CMC:PVOH/SB	5.06 (0.05)	+	33.04
	CMC:PVOH/SB UV	4.47 (0.09)	+	25.83
E. Coli	CMC:PVOH	0.00 (0.00)	-	
	CMC:PVOH/SB	4.59 (0.15)	+	27.22
	CMC:PVOH/SB UV	3.54 (0.34)	+	16.14
Candida spp.	CMC:PVOH	0.00 (0.00)	-	
	CMC:PVOH/SB	*Complete inhibition*	+	100
	CMC:PVOH/SB UV	*Complete inhibition*	+	100
Penicillium spp*.*	CMC:PVOH	0.00 (0.00)	-	
	CMC:PVOH/SB	3.65 (0.07)	+	17.18
	CMC:PVOH/SB UV	5.48 (0.10)	+	9.01

+: represents an inhibitory; **-**: represent no inhibitory effect,

* Values are measurements of diameter of inhibitory zone and expressed in cm. The values in parentheses correspond to the standard deviation.

** Contact area is the part of agar on Petri dish directly underneath film pieces.

Graphical abstract

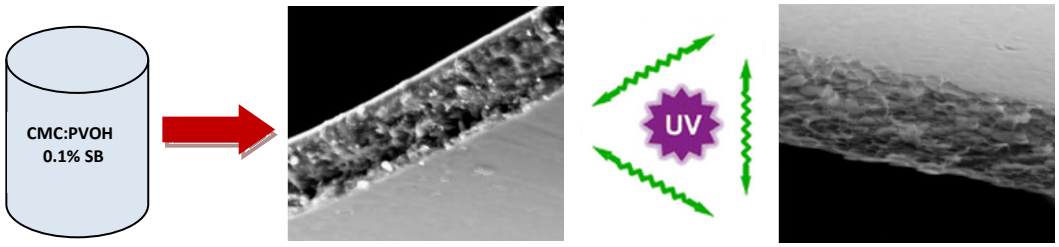

HIGHLIGHTS

CMC:PVOH blend films were developed with the addition of sodium benzoate (SB)

Exposition to UV radiation was carried out with sodium benzoate as photoinitiator Blend films were exposed to UV radiation to modify their surface morphology

Low O_2 permeability of UV treated blends allow them to be used as selective packaging

Efficacy of SB as an antimicrobial agent was examined with and without UV radiation